Marine-Derived Water-Soluble Organic Nitrogen in Coastal Air: Influence of Ocean Productivity on Atmospheric Nitrogen Cycling

Jiao Tang[1,2], Shujie Hu[3*]; Xiao Wang[4]; Jiaqi Wang[5], Shaojun Lv[2]; Xiaofei Geng[2]; Guangcai Zhong[2], Yangzhi Mo[2], Surat Bualert[6], Jun Li[2], Shizhen Zhao[2*]; Gan Zhang[2]

[1] College of Marine Sciences, South China Agricultural University, Guangzhou 510642, China

[2] State Key Laboratory of Advanced Environmental Technology, Guangzhou Institute of Geochemistry, Chinese Academy of Sciences, Guangzhou, 510640, China

[3] Chongqing Institute of Green and Intelligent Technology, Chinese Academy of Sciences, Chongqing, 400714, China

[4] School of Resources and Environment, Henan Polytechnic University, Jiaozuo 454003, China

[5]School of Electrical and Information Engineering, Zhengzhou University, Zhengzhou, 450001, China

[6]Faculty of Environment, Kasetsart University, Bangkok, 10900, Thailand

***Correspondence to**: Shujie Hu (hushujie@cigit.ac.cn) and Shizhen Zhao (zhaoshizhen@gig.ac.cn)

Abstract

Organic nitrogen (ON) deposition from aerosols plays a crucial role in oceanic ecosystems; however, the influence of marine biogenic activity on atmospheric ON remains poorly understood. Here, we investigate the contribution of the marine biosphere to water-soluble ON (WSON) in coastal aerosols based on particulate matter samples collected in Bangkok, Thailand, from January 2016 to January 2017. Concentrations of WSON and water-soluble inorganic nitrogen (WSIN, including NO_3^- and NH_4^+) were analyzed and compared across days classified by air mass origin over land as marine-, mixed-, or continental-influenced. Air masses of marine origin showed significantly lower WSON and WSIN concentrations than those from mixed and continental origins. Nevertheless, WSON remained a substantial fraction of water-soluble total nitrogen (WSTN) across all air-mass categories, although the WSON/WSTN ratio alone did not uniquely distinguish marine from anthropogenic influence. Positive matrix factorization revealed that the contribution of sea spray aerosol (SSA)-associated WSON to total WSON increased markedly with oceanic influence, accounting for 3.8% ± 6.4%, 14% ± 14%, and 34% ± 17% under continental, mixed, and marine conditions, respectively. The corresponding contributions to WSTN were approximately 1.6% ± 2.1%, 7.3% ± 7.6%, and 13% ± 8.2%, with an overall mean of 7.8% ± 8.2% over the sampled annual cycle. Moreover, marine productivity, assessed via air mass exposure to chlorophyll-a concentrations, exhibited a strong positive correlation with SSA-associated WSON ($r = 0.96$, $p < 0.001$), a pattern further supported by large-scale comparison across coastal sites. These results provide multiple lines of evidence that SSA-associated WSON is an important contributor to coastal aerosol WSON under marine influence, with patterns consistent with marine-biogenic enhancement, although anthropogenic co-influences cannot be fully excluded.

1. Introduction

Organic nitrogen (ON), which includes compounds such as amino acids, urea, organic nitrates, nitroaromatics, and humic-like substances, plays an important role in atmospheric processes including air quality, cloud formation, and the nitrogen cycle (Cape *et al.*, 2011). On a global scale, water-soluble ON (WSON) has been estimated to contribute 10%–40% of total airborne ON (Cape *et al.*, 2011; Liu *et al.*, 2021; Matsumoto *et al.*, 2019a), influencing aerosol properties such as solubility, acidity, and hygroscopicity. Furthermore, certain nitrogen-containing organic compounds, including nitroaromatics, have been recognized as important chromophores in brown carbon (He *et al.*, 2022; Liu *et al.*, 2023), thereby influencing radiative forcing. In addition, atmospheric deposition of particulate WSON is increasingly regarded as a significant source of nitrogen input to marine ecosystems (Buchanan *et al.*, 2021; Li *et al.*, 2023).

WSON originates from both direct emissions—including anthropogenic and biogenic sources—and secondary formation through atmospheric reactions (Xu *et al.*, 2020; Yu *et al.*, 2017). These complex sources and atmospheric processes contribute to substantial spatial and temporal variability in WSON deposition (Kanakidou *et al.*, 2012; Li *et al.*, 2023; Yu *et al.*, 2020). Previous studies have identified marine emissions as a notable source of atmospheric ON (Facchini *et al.*, 2008; O'Dowd *et al.*, 2004). Globally, the estimated annual primary emission of soluble ON from the ocean is 2.1 Tg N yr^{-1}, comparable in magnitude to anthropogenic emissions from fossil fuel combustion and biomass burning (BB) (Ito *et al.*, 2014; Kanakidou *et al.*, 2012). In some remote marine regions, isotopic evidence suggests that aerosol ON can be strongly influenced by marine biological production rather than terrestrial pollution (Altieri *et al.*, 2016).

Recent research has underscored the complexity and variability of WSON in sea spray aerosol (SSA) (Altieri *et al.*, 2012; Li *et al.*, 2019). For instance, primary emissions of sea-spray emissions have been recognized as a major source of WSON over the remote Indian sector of the Southern Ocean (Matsumoto *et al.*, 2022). These findings highlight the importance of incorporating marine ON emissions in assessments of net atmospheric WSON deposition, particularly in the open ocean (Luo *et al.*, 2018). However, several field studies in regions strongly influenced by marine air masses have reported only minor contributions from marine-derived WSON—typically below 5%

(Leung *et al.*, 2024; Tsagkaraki *et al.*, 2021). This discrepancy highlights the continuing challenge of distinguishing marine from anthropogenic WSON sources in coastal and adjacent marine environments. In this study, we address this issue by combining Positive Matrix Factorization (PMF) source apportionment, air-mass trajectory analysis, a trajectory-based land-retention index, and chlorophyll-a (Chl-a) exposure as complementary lines of evidence, while recognizing that these approaches reduce but do not fully eliminate source ambiguity.

The Indochinese Peninsula (ICP), characterized by high population density and substantial ON deposition (Ito *et al.*, 2014; Kanakidou *et al.*, 2012; Li *et al.*, 2023), provides a suitable context for assessing the influence of marine aerosols on atmospheric WSON. Eutrophication, defined as the excessive enrichment of aquatic systems by nutrients that alters ecosystem structure and function, may enhance primary productivity and potentially promote the emission of ON to the atmosphere (Altieri *et al.*, 2016). Here, we selected Bangkok, the capital of Thailand, which is situated in the central plain of the country and adjacent to the Gulf of Thailand. The region experiences prevailing marine winds from January to October, offering a favorable setting for studying marine aerosol contributions to WSON. Our study aims to: (1) quantify WSON abundances at a coastal site in the ICP; (2) assess marine influences on WSON distributions; and (3) elucidate the mechanisms governing oceanic contributions to WSON.

2. Material and Methods

2.1. Sampling Campaign

A total of 84 total suspended particulate (TSP) samples were collected from the rooftop (57 m above ground level) of the Faculty of Environment at Kasetsart University (100°57′ E and 13°85′ N; Figure 1a) in Bangkok, Thailand—a site previously characterized in air quality studies (Tang *et al.*, 2021; Wang *et al.*, 2020). Sampling was conducted over 24-hour periods using a high-volume air sampler (flow rate: 0.3 m^3 min^{-1}) equipped with pre-combusted quartz-fiber filters (450 °C for 6 h). The collection period spanned from 18 January 2016 to 28 January 2017, covering three distinct seasons: Dry I (January–March 2016, n = 19), Wet (April–June and October 2016, n = 35), and Dry II (November 2016–January 2017, n = 30). Sampling frequency averaged 5 ± 2 days per month during January–February 2016 and January 2017, with

intensified campaigns in March–May and late October–December. Sampling was limited between June and October due to heavy rainfall. Because the sampling frequency varied among seasons and was reduced during the rainy period, this dataset does not represent a uniformly sampled annual climatology. Accordingly, the results are interpreted as observation-based estimates for the sampled annual cycle, and caution is needed when extending them to annual-scale representativeness. Precipitation and solar radiation data were obtained from historical reanalysis products provided by the European Centre for Medium-Range Weather Forecasts (ECMWF). All samples and field blanks were stored in the dark at –20 °C until analysis. This storage procedure helps minimize post-collection changes, but it does not eliminate artifacts generated during sampling itself. A summary of TSP mass concentrations, chemical components, and meteorological conditions is provided in Table S1 (*Supplement*).

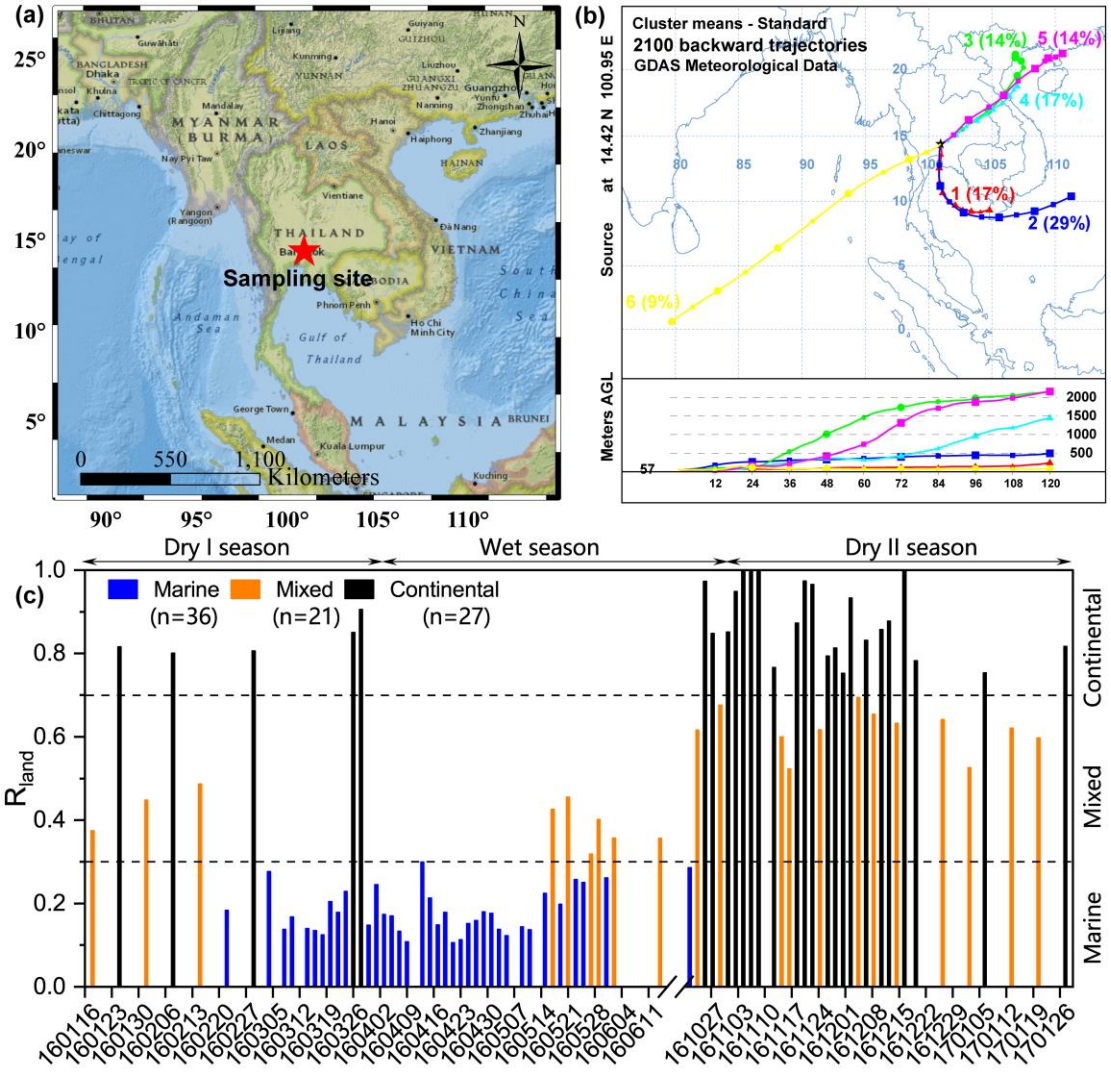

Figure 1. (a) Sampling site location in Bangkok, Thailand. (b) Classified air mass trajectories (detailed in Figure S1–S2). (c) Distribution of R_{land}, with samples categorized as marine-influenced (R_{land} < 0.3), mixed-influenced (0.3 ≤ R_{land} ≤ 0.7), or continental-influenced (R_{land} > 0.7) based on the R_{land} values. The map in panel (a) was created using ArcGIS software with the base layer from the ESRI National Geographic World Map.

2.2. Chemical Analysis

Organic carbon (OC) and elemental carbon (EC) mass concentrations were determined using an OC/EC analyzer following the NIOSH 870 thermal-optical protocol. Inorganic ions (Cl^-, NO_3^-, SO_4^{2-}, Na^+, K^+, NH_4^+, Mg^{2+}, and Ca^{2+}) were quantified by ion chromatography (761 Compact IC, Metrohm, Switzerland), and trace elements were analyzed via inductively coupled plasma–mass spectrometry (ICP–MS; ELAN DRC II, PerkinElmer Ltd., Hong Kong). Analytical errors were 5.5% for OC, and 3.9% for EC, below 5.0% for trace elements, and under 1.0% for water-soluble ions, based on prior validation (Wang *et al.*, 2020).

Polar molecular tracers—including BB markers (levoglucosan, mannosan, galactosan) and biogenic/anthropogenic secondary organic aerosol (SOA) tracers such as 2-methylglyceric acid (2-MGA), 2-methylthreitol and 2-methylerythritol (2-MGL), 3-methyl-1,2,3-butanetricarboxylic acid (MBTCA), and o/p-phthalic acid—were analyzed by gas chromatography–mass spectrometry (GC–MS) following derivatization as previously reported (Geng *et al.*, 2020; Li *et al.*, 2013). The mean recovery of ^{13}C-labeled levoglucosan was 87% ± 10%. Non-polar tracers of coal and fossil fuel combustion (hopanes and steranes) were also analyzed, with perdeuterated tetracosane yielding a recovery of 114% ± 11% (Wang *et al.*, 2020).

Water-soluble OC (WSOC) and water-soluble total nitrogen (WSTN) were extracted by ultrasonication for 30 minutes using ultrapure water (resistivity > 18.2 MΩ cm), followed by filtration through 0.22 μm PTFE membranes. Concentrations were measured with a TOC/TN analyzer (model TOC-Vcsh, Shimadzu). WSON was calculated as the difference between WSTN and water-soluble inorganic nitrogen (WSIN), where WSIN comprises NH_4^+-N, NO_3^--N, and NO_2^--N: [WSON] = [WSTN] − [WSIN]. Nitrite concentrations were consistently below the detection limit of ion chromatography and were excluded from further analysis. It should be noted that some dissolved ON species may

not be fully converted to nitrogen monoxide in the TOC/TN analyzer, potentially leading to underestimation of WSON (Miyazaki *et al.*, 2011). Furthermore, integrated filter sampling may be affected by gas–particle sampling artifacts, including volatilization losses of semi-volatile inorganic nitrogen species and possible adsorption of gaseous nitrogen compounds on the filter. Previous studies suggested that adsorption of gaseous organics onto quartz filters may have only a limited effect on WSON measurement under similar sampling conditions, whereas volatilization loss during sampling may still lead to underestimation of particulate WSON (Matsumoto *et al.*, 2014; Matsumoto and Yamato, 2016).

The relative standard deviation (RSD) for WSTN analysis was 3.6% (method) and 0.77% (instrument). Method detection limits were 0.09 μg m^{-3} for WSON, 0.03 μg m^{-3} for NO_3^-, and 0.02 μg m^{-3} for NH_4^+. Field blank levels were 0.067 μgN m^{-3} (WSON), 0.043 μgN m^{-3} (NH_4^+-N), and 0.07 μgN m^{-3} (NO_3^--N), corresponding to average blank-to-sample ratios of 7.1%, 4.3%, and 12%, respectively, consistent with previous reports (Matsumoto *et al.*, 2019a). All reported WSON and WSTN concentrations were blank-corrected and should be interpreted as operationally defined particulate water-soluble N concentrations under the applied sampling protocol.

2.3 Source Apportionment

The U.S. Environmental Protection Agency's PMF model (PMF 5.0) was employed to perform factor analysis on environmental data with non-negativity constraints and to estimate associated uncertainties (Norris *et al.*, 2014). PMF has been widely applied as a robust tool for aerosol source apportionment. In PMF 5.0, species are evaluated based on the signal-to-noise (S/N) ratio and can be classified as "strong," "weak," or "bad". Weak species are retained but assigned a tripled uncertainty, whereas bad species are excluded from the modeling. In this study, WSON was included as a total variable to resolve its sources. Following the base run, rotational stability (F_{peak}) tests were conducted, and model robustness was evaluated using the base model displacement (DISP), bootstrap (BS), and bootstrap displacement (BS-DISP) methods. A detailed description of PMF procedures is provided in Text S1 in *Supplement*.

2.4. Air Mass Back Trajectories and Trajectory-Based Chl-a Exposure.

To identify potential source regions, we calculated 120-hour back

trajectories using the Hybrid Single-particle Lagrangian Integrated Trajectory (HYSPLIT) model (http://www.arl.noaa.gov/HYSPLIT.php), driven by the Global Data Assimilation System (GDAS) meteorological dataset at 1° × 1° resolution (http://ready.arl.noaa.gov/archives.php). Trajectories were generated at 1-hour intervals and subsequently classified through cluster analysis (Figure 1b and Figures S1–S2). Based on origin and transport pathways, air masses arriving in Bangkok were grouped into six distinct clusters. During the Dry I season, air masses originated predominantly over the Gulf of Thailand/South China Sea (clusters 1–2), with a minor contribution from the Indochina Peninsula (cluster 3). In the Wet season, trajectories were primarily transported via the South China Sea/Gulf of Thailand and the Arabian Sea (clusters 1, 2, 6), whereas Dry II season air masses mainly originated over mainland China and crossed the Indochina Peninsula (clusters 3–5).

Furthermore, the air mass retention ratio over land (R_{land}), defined as the weighted ratio of transport time over land to the total transport duration, was calculated according to the method of Zhou *et al.* (2021, 2023) using Equation 1. This parameter provides a quantitative measure of terrestrial influence at the receptor site. A schematic illustration is presented in Figure S3.

$$R_{land} = \frac{\sum_{i=1}^{N_{land}} e^{-t_i/120}}{\sum_{i=1}^{N_{total}} e^{-t_i/120}} \quad (1)$$

Here, N_{total} denotes the total number of trajectory endpoints and N_{land} the number over land. The backward tracking time t_i (in hours) and the weighting factor $e^{-t_i/120}$ account for the diminishing influence of distant regions due to air mass diffusion and particle deposition during transport. As a result, regions associated with longer backward tracking times exert a weaker influence on the receptor site compared to nearby areas. Based on the R_{land} values (Figure 1c), samples were categorized as marine-influenced ($R_{land} < 0.3$), mixed-influenced ($0.3 \leq R_{land} \leq 0.7$), or continental-influenced ($R_{land} > 0.7$). It should be noted that marine-influenced air masses, as defined by low R_{land}, do not necessarily represent purely marine-biogenic conditions, because aged marine aerosol, shipping emissions, and anthropogenically polluted air masses transported over the ocean may also contribute to aerosol composition. This classification is further supported by molecular marker analysis: during marine-influenced periods, the regression slope for Na^+ with Mg^{2+} (0.11) closely aligned

with the seawater reference ratio (0.12). Elevated levels of Cl^-, Na^+, Mg^{2+}, and the $Na^+/\sum ions$ ratio consistently reflected enhanced sea-salt influence during marine-influenced periods. By contrast, non-sea-salt sulfate (nss-SO_4^{2-}) was not interpreted here as a unique indicator of marine origin, because it may include contributions from both anthropogenic sulfur and marine biogenic sulfur and may also reflect secondary atmospheric processing during transport (Savoie *et al.*, 2002). Particulate NO_3^- was mainly interpreted as a secondary product formed from the oxidation of NO_x emitted by combustion-related sources, including traffic, shipping, industrial activities, and fossil-fuel or BB, followed by gas-to-particle partitioning or heterogeneous reactions with sea-salt particles during transport (Pryor and Sørensen, 2000). Its concentration was lowest during marine-influenced periods, lower than under mixed- and continental-influenced conditions, a pattern consistent with combustion-derived species such as non-sea-salt K^+ (nss-K^+), EC, and levoglucosan. These results indicate reduced, but not absent, terrestrial and anthropogenic influence during marine-influenced periods (Table S2).

Air mass exposure to Chl-a (AEC), defined as the mean sea surface Chl-a concentration along air mass trajectories, was used as a proxy for marine biogenic emissions at the receptor site (Park *et al.*, 2018; Zhou *et al.*, 2023). A statistically significant positive correlation was observed when air masses traveled within the marine boundary layer. However, due to the relatively low correlation between AEC and methanesulfonate, the formulation was adjusted based on the approach of Zhou *et al.* (2021, 2023), as follows:

$$AEC = \frac{\sum_{i=1}^{N_{total}} Chl\text{-}a_i \cdot e^{-t_i/120} \cdot e^{-h_i/500}}{n} \quad (2)$$

Here, N_{total} denotes the total number of hourly endpoints (120, including the receptor point) along the trajectory. The variable $Chl\text{-}a_i$ represents the mean Chl-a concentration—derived from MODIS-Aqua monthly composites at a 4 km resolution—within a 20 km radius of the i_{th} trajectory endpoint. Endpoints over land were assigned $Chl\text{-}a_i$ = zero. The weighting factor $e^{-h_i/500}$ accounts for the influence of altitude h_i, reflecting the reduced contribution from higher altitudes due to Chl-a dilution and particle deposition during transport. The denominator n corresponds to the number of trajectory endpoints with valid Chl-a data, including zero values over land.

2.5. Potential Source Contribution Function (PSCF) Model

The PSCF model was employed to identify source regions by discretizing the study domain into an $i \times j$ grid. The PSCF values, ranging from 0 to 1, represent the conditional probability that an air parcel passing through a grid cell contributes to high concentrations at the receptor site; elevated values denote a higher probability of source contribution. In this study, PSCF analysis was applied to identify potential geographic source regions of both total WSON and PMF-resolved source categories of WSON in aerosols collected in Bangkok. A detailed description of the PSCF methodology is provided in Text S2 and in previous publications (Geng *et al.*, 2020; Tang *et al.*, 2024).

3. Results and Discussion

3.1. Temporal Variations of WSON

Figure S4 and Table S1 present the temporal variations and statistical summaries of meteorological parameters and chemical compositions in TSP throughout the sampling campaign. In Bangkok, Thailand, the mass concentrations of TSP, OC, and EC were 55 ± 30 μg m^{-3} (17–161 μg m^{-3}), 12 ± 6.3 μg m^{-3} (3.7–38 μg m^{-3}), and 1.4 ± 0.43 μg m^{-3} (0.16–2.8 μg m^{-3}), respectively. The TSP levels in this region were substantially lower than those reported in other areas, such as the Eastern Mediterranean (220 ± 105 μg m^{-3}; Tripathee *et al.*, 2021), Jiaozhou Bay (134 ± 80 μg m^{-3}; Xing *et al.*, 2018), and Xi'an during the dust episodes (2109 ± 1360 μg m^{-3}; Wang *et al.*, 2014). Pronounced seasonal variations were observed: TSP levels decreased by 56% from the Dry I season to the Wet season, but increased by 52% during the Dry II season. In Bangkok, rainfall during the Wet season (April to October) accounted for 92% of the annual precipitation total. To examine wet scavenging effects, we evaluated the relationship between TSP concentrations and precipitation (Figure S5a). A significant negative correlation was identified ($R^2 = 0.22$, $p < 0.001$), consistent with a contribution from wet scavenging, although the relatively low explanatory power indicates that emissions, transport, and precipitation history along the air-mass pathway also substantially influenced TSP variability.

The mass fraction of WSTN in TSP collected in Bangkok averaged 3.8% ± 1.1% (2.2%–7.2%), which was somewhat higher than that reported in the Eastern Mediterranean (~ 2.7%; Tripathee *et al.*, 2021) and comparable to

values from Sapporo, Japan (3.8% ± 2.3%; Pavuluri *et al.*, 2015). As shown in Figure 2a and Table S2, the concentrations of the individual WSTN components, including WSON, NO_3^--N, and NH_4^+-N, were 0.95 ± 0.40 μgN m^{-3} (0.27–2.3 μgN m^{-3}), 0.60 ± 0.52 μgN m^{-3} (below detection limitation (BDL)–2.7 μgN m^{-3}), and 0.47 ± 0.44 μgN m^{-3} (BDL–2.2 μgN m^{-3}), respectively. WSON correlated positively with both TSP ($r = 0.65$, $p < 0.01$) and WSIN ($r = 0.51$, $p < 0.01$) (Figure S6), indicating that WSON variability was linked to overall aerosol loading and co-varied with inorganic N across the dataset.

Concentrations of WSON, NO_3^--N, NH_4^+-N, TSP, OC, and EC varied considerably under different air mass regimes (Table S2). The nonparametric Mann–Whitney U test indicated that WSON and NO_3^--N levels were significantly lower during marine-influenced periods than under mixed or continental conditions (Figure 2c, $p < 0.001$). In contrast, NH_4^+-N concentrations were slightly higher during marine periods. This contrast indicates that the responses of individual N species were not uniform across air-mass regimes and should not be attributed to a single dominant source. This aligns with earlier studies reporting that aerosols in remote marine regions may still be substantially influenced by continental inputs (Jickells *et al.*, 2013). BB tracers (e.g., levoglucosan, galactosan, mannosan) were also significantly lower during marine-influenced days (see Table S2). Furthermore, WSON correlated with BB and SOA markers and aerosol liquid water content (ALWC, Text S3) under mixed and continental conditions, whereas these associations were not evident during marine periods (Figure S7). Taken together, these patterns suggest that the lower WSON concentrations during marine-influenced periods likely reflected a combination of reduced continental and combustion-related influence, differences in transport history, and atmospheric processing. Seasonally higher rainfall may also have contributed, but because no significant direct correlation was found between WSON and precipitation (Figure S5b), precipitation alone cannot explain the observed WSON variability.

The WSON/WSTN ratio during marine-influenced days (50% ± 17%) was similar to that under continental influence (48% ± 15%) but lower than during mixed conditions (60% ± 17%) (Figure 2d). This pattern shows that the WSON/WSTN ratio alone may not be a reliable way to identify the source of this dataset. The elevated ratio under mixed conditions likely reflects overlapping marine and continental influences together with different responses

of WSON and WSIN to transport and removal processes, rather than a unique source type. During marine-influenced periods, WSON may reflect both marine-related contributions and anthropogenic inputs associated with shipping emissions and atmospheric processing, whereas continental periods are more strongly affected by terrestrial anthropogenic emissions. Precipitation may alter the WSON/WSTN ratio through differential scavenging: WSIN species (e.g., NO_3^-, NH_4^+) are efficiently removed by rainfall (Matsumoto *et al.*, 2019b; Nehir and Koçak, 2018), as WSIN showed stronger correlations with precipitation (Figure S5c,d). By contrast, the absence of a significant WSON–precipitation correlation indicates that WSON variability in this dataset was less directly coupled to precipitation, rather than supporting a distinct scavenging mechanism.

Annually, WSON accounted for 52% ± 17% of the WSTN (Figure 2b)—substantially higher than values reported from a forest site (20% ± 11%; Miyazaki *et al.*, 2014), an offshore island (27%; Tian *et al.*, 2023), Sapporo (9.2% ± 7.3%; Pavuluri *et al.*, 2015), and coastal Qingdao (~20%; Shi *et al.*, 2010). Elevated WSON/WSTN ratios have been documented in source emissions such as BB (80% ± 6.3%), vehicle exhaust (67% ± 16%), and shipping emissions (54% ± 31%) (Yu *et al.*, 2017), as well as receptor regions such as Hawaii (64%; Cornell *et al.*, 2001) and polluted continental urban regions such as Xi'an (45%, range: 22%–68%; Ho *et al.*, 2015). By comparison, the South China Sea, which is more strongly influenced by open-marine conditions, exhibited a WSON/WSTN ratio of 34%, whereas the Yellow Sea, subject to stronger continental and anthropogenic influence, showed a lower ratio of 17% (Shi *et al.*, 2010). During phytoplankton blooms, ON can dominate aerosol composition, contributing up to 84% of WSTN (Violaki *et al.*, 2015) and 63% of submicrometer aerosol mass (O'Dowd *et al.*, 2004). Collectively, these studies indicate that elevated WSON/WSTN ratios may arise from anthropogenic combustion sources, shipping emissions, marine-related emissions, and secondary atmospheric processing. Therefore, the WSON/WSTN ratio alone is insufficient to discriminate marine-biogenic, shipping-related, and continental anthropogenic sources of WSON. More quantitative approaches are needed to apportion the origins of aerosol ON.

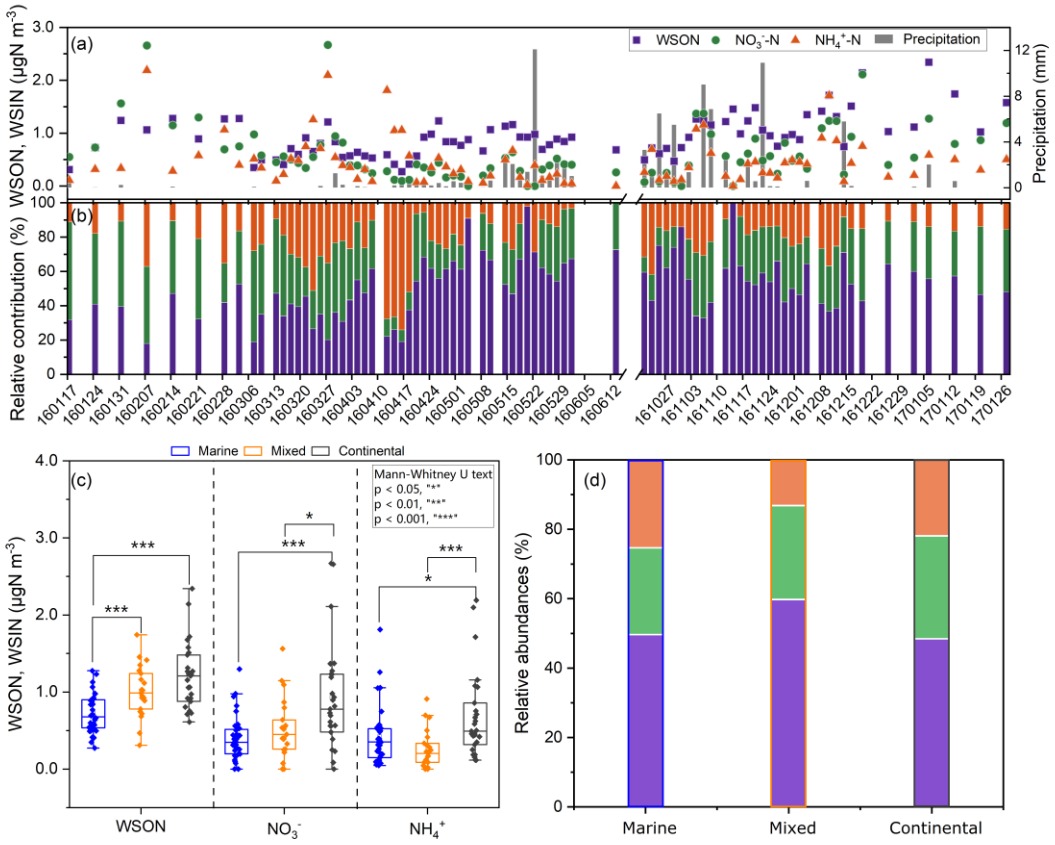

Figure 2. Temporal variations and source influences on N species in Bangkok aerosols. (a) Time-series of concentrations of WSON and WSIN (NH_4^+-N, NO_3^--N), overlaid with daily rainfall from ECMWF reanalysis data. (b) Relative contributions of WSON and WSIN to WSTN across the study period. (c) Concentration distributions and (d) relative abundances of WSON and WSIN during marine-, mixed-, and continental-influenced periods.

3.2. SSA as a Major WSON Source in Marine-influenced Days

To elucidate the contributions of marine and anthropogenic sources to WSON in this coastal urban environment, we applied the PMF 5.0 model to 84 aerosol samples characterized by 26 chemical species. The model resolved WSON into seven source factors: shipping emissions, secondary sulfate, dust, SOA, BB, vehicle emissions and fossil-fuel combustion (VEFC), and SSA (Figure S8); the detailed identification of each factor is provided in Text S1. The SSA factor was characterized primarily by high loadings of Na^+, Cl^-, and Mg^{2+}, with WSON also contributing to this factor. We therefore interpret this factor as a sea-salt-associated aerosol carrying WSON, rather than as purely biogenic aerosol. Furthermore, PSCF mapping of SSA-associated WSON pointed

mainly to the Gulf of Thailand and, to a lesser extent, the Bay of Bengal (see Figure S10), supporting the importance of marine-related source regions for this factor.

Over the entire study period, SOA (34% ± 25%), VEFC (21% ± 16%), SSA (19% ± 19%), and BB (13% ± 12%) emerged as the dominant sources of WSON in Bangkok aerosols (Figures 3b and S9). This is consistent with previous reports highlighting secondary formation and BB as major contributors to WSON (Leung *et al.*, 2024; Tsagkaraki *et al.*, 2021; Yu *et al.*, 2017). Earlier factor-based studies also indicated that sea salt can explain over 20% of the variance in WSON (Chen and Chen, 2010; Shi *et al.*, 2010). The contribution of SSA in our study, however, exceeded values reported for other coastal regions such as Hong Kong (4.4%) and the Eastern Mediterranean (<5%) (Leung *et al.*, 2024; Nehir and Koçak, 2018; Tsagkaraki *et al.*, 2021). Two factors may explain this discrepancy. First, ON in coarse aerosols often originates from soil, dust, or large sea-salt particles (Cornell *et al.*, 2001; Mace *et al.*, 2003), whereas studies focusing on $PM_{2.5}$—such as those in Hong Kong—naturally record lower sea-salt contributions (Leung *et al.*, 2024). Second, the ultra-oligotrophic marine environment of the Eastern Mediterranean, characterized by low nutrient availability and limited riverine input, results in low marine productivity and thus diminished marine-derived WSON (Nehir and Koçak, 2018; Tsagkaraki *et al.*, 2021).

We further disaggregated WSON source contributions by air mass regime (Figure 3b). Under marine influence, SSA constituted the dominant source of WSON (34% ± 17%), exceeding SOA (19% ± 17%), VEFC (19% ± 14%), and secondary sulfate (17% ± 16%), while BB contributed minimally (7.1% ± 6.0%). This pattern is consistent with studies conducted in remote marine and island settings (Altieri *et al.*, 2016; Miyazaki *et al.*, 2011; Violaki *et al.*, 2015). Under mixed marine–continental influence, SOA became the dominant contributor (51% ± 20%), followed by VEFC (19% ± 14%) and SSA (14% ± 15%). During continental conditions, SOA remained the primary source (41% ± 26%), likely reflecting multiple secondary formation pathways of nitrogen-containing organic aerosol, of which nitroaromatics may represent one possible subset of these compounds (Xie *et al.*, 2017). Previous work has shown that oxidized *α*-pinene SOA can account for 33%–38% of WSON, with aerosol liquid water further promoting nighttime secondary WSON formation (Xu *et al.*, 2020). Under

continental regimes, VEFC (26% ± 19%) and BB (23% ± 14%) also contributed substantially to WSON. Notably, the SSA contribution dropped sharply to 3.8% ± 6.4% under continental influence. Expressed relative to total WSTN, SSA-associated WSON contributed approximately 1.6% ± 2.1%, 7.3% ± 7.6%, and 13% ± 8.2% under continental-, mixed-, and marine-influenced conditions, respectively, with an overall mean contribution of 7.8% ± 8.2% over the sampled annual cycle, further illustrating its enhanced importance during marine influence.

Temporal variations in source-resolved WSON concentrations are shown in Figure 3a. Among the three air mass regimes, SSA-associated WSON concentrations peaked under marine influence (0.19 ± 0.12 μgN m^{-3}), approximately 1.7 times higher than during mixed periods (0.11 ± 0.12 μgN m^{-3}) and five times higher than during continental periods (0.037 ± 0.069 μgN m^{-3}). Shipping-emission-associated WSON was also elevated during marine days (0.015 ± 0.0075 μgN m^{-3}) relative to mixed and continental periods, though its overall contribution remained low (~3%). WSON associated with the secondary sulfate factor under marine influence (0.094 ± 0.086 μgN m^{-3}) was significantly higher than during mixed periods (0.022 ± 0.023 μgN m^{-3}) and during continental periods (0.046 ± 0.056 μgN m^{-3}), consistent with an important contribution from secondary inorganic aerosol formation. Although the PMF-resolved shipping factor remained low during marine-influenced periods, other anthropogenic-related factors, including secondary sulfate, VEFC and SOA factor, still showed non-negligible contributions, consistent with the view that marine-influenced air masses in this study should not be interpreted as purely marine-biogenic conditions. These results also indicate that marine air mass transport plays an important role in the enhancement of SSA-associated WSON, further supported by a strong negative correlation between SSA-associated WSON and R_{land} (Figure 3c, $r = -0.59$, $p < 0.001$). In contrast, SOA-, BB-, and VEFC-associated WSON increased significantly under mixed and continental conditions. Although SOA is generally considered more susceptible to wet removal than primary aerosol (Sun *et al.*, 2011; Zhao *et al.*, 2026), no significant correlation was observed between precipitation and PMF-resolved source concentrations in this dataset. This suggests that wet scavenging alone did not dominate the observed source-resolved WSON variability.

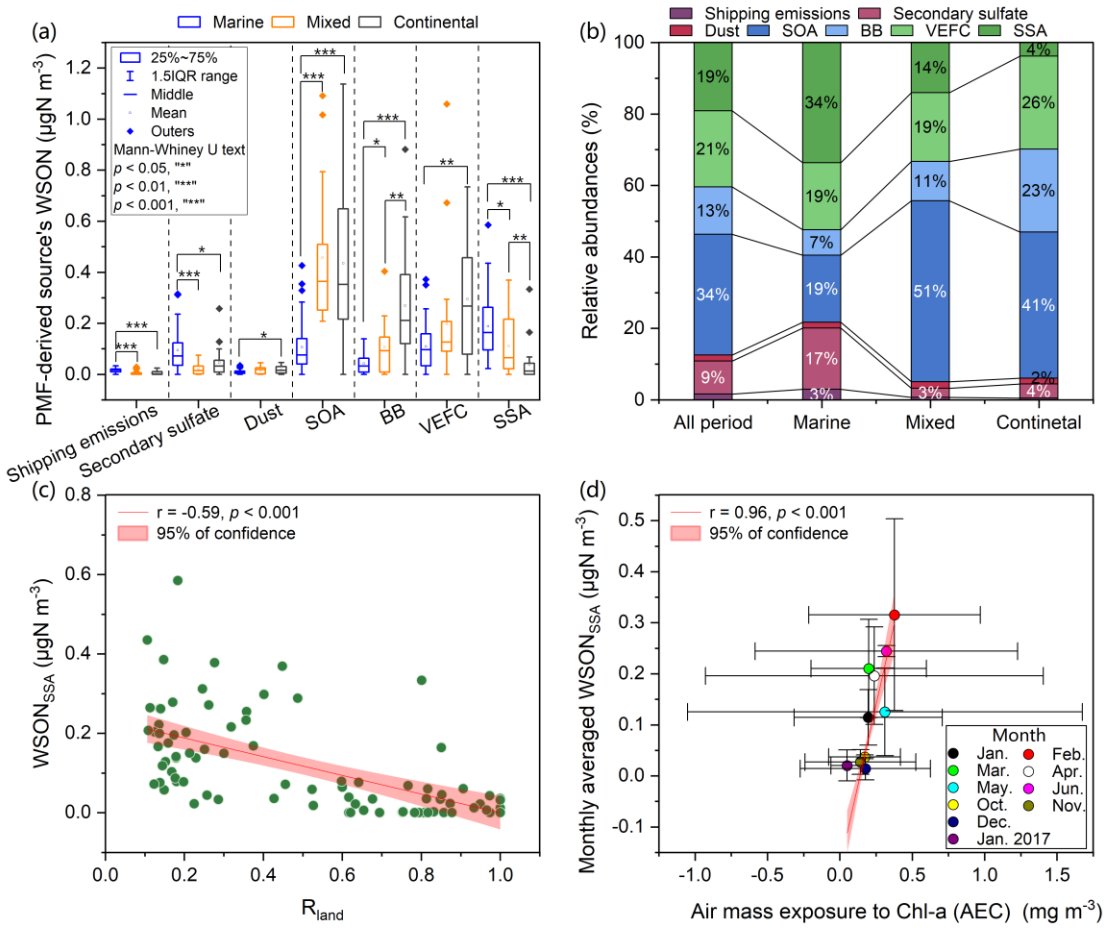

Figure 3. Source apportionment of WSON based on PMF. (a) Absolute concentrations and (b) relative contributions of PMF-resolved sources to total WSON during the entire study period and under marine-, mixed-, and continental-influenced conditions. (c) Correlation between R_{land} and SSA-associated WSON. (d) Relationship between AEC and monthly averaged SSA-associated WSON concentrations, color-coded by sampling month.

3.3. Marine Productivity as a Key Factor influencing Coastal WSON Distribution

SSA is dominated by inorganic sea salt but can also comprise an important organic fraction derived from ocean-surface materials (Prather *et al.*, 2013; Quinn *et al.*, 2014; Schiffer *et al.*, 2018). Previous studies have linked marine biological productivity to the organic enrichment of SSA (O'Dowd *et al.*, 2015; Violaki *et al.*, 2015), and Chl-a has often been used as a broad proxy for ocean-surface biological conditions (Facchini *et al.*, 2008; O'Dowd *et al.*, 2004). Given the substantial contribution of SSA-associated WSON to total WSON and WSTN during marine-influenced periods in our study, we further examined whether marine productivity was related to its variability.

We calculated AEC values based on monthly MODIS Chl-a data (4 km resolution) along 120-hour backward trajectories (see Methods). SSA-associated WSON exhibited a strong positive correlation with AEC ($r = 0.96$, $p < 0.001$; Figure 3d), consistent with a linkage between marine productivity and the variability of this factor. This contrasts with Tian *et al.* (2023), who observed significant WSON-AEC correlations only in summer, likely reflecting stronger anthropogenic influences and/or weaker marine signals during other seasons. While previous multivariate regression identified wind speed and Chl-a as key predictors of the organic fraction in SSA (Gantt *et al.*, 2011), other studies note that Chl-a alone may not fully capture organic enrichment (Rinaldi *et al.*, 2013). Still, moderate correlations ($r \approx 0.60$) between Chl-a and marine organic aerosol abundance have been reported (Sciare *et al.*, 2009). However, AEC may also covary with marine transport conditions, meteorology, and other seasonally structured processes, and correlation alone does not establish source dominance. Taken together, the PMF results, reduced terrestrial influence, and the positive AEC relationship are consistent with an important marine-biogenic enhancement of SSA-associated WSON during marine-influenced periods, although shipping and other anthropogenic co-influences cannot be fully excluded.

To further examine the broader relevance of this relationship, we compiled a dataset of WSON concentrations from coastal and island sites and recalculated air-mass trajectories, R_{land}, and AEC values based on MODIS Chl-a for each site (Figure 4a and Table S3). Across these marine-influenced coastal datasets, the highest WSON concentrations occurred at Huaniao Island (Tian *et al.*, 2023), followed by Jiaozhou Bay (Xing *et al.*, 2018), Hong Kong (Ho *et al.*, 2019; Leung *et al.*, 2024), the South China Sea (Shi *et al.*, 2010), and Bangkok. The lowest values were observed in the Eastern Mediterranean (Tsagkaraki *et al.*, 2021), Keelung City (Chen and Chen, 2010), Okinawa Island (Kunwar and Kawamura, 2014), Barbados (Zamora *et al.*, 2011), and Sapporo (Pavuluri *et al.*, 2015). Notably, spatial patterns in AEC closely mirrored those in WSON. A significant positive correlation was found between WSON and AEC across all sites ($r = 0.82$, WSON [nmol m^{-3}] = 276 × AEC [mg m^{-3}] – 2.74, Figure 4b). This large-scale comparison supports the broader consistency of the observed relationship, although the influence of site-to-site differences in sampling protocol, aerosol size fraction, and anthropogenic impact cannot be excluded.

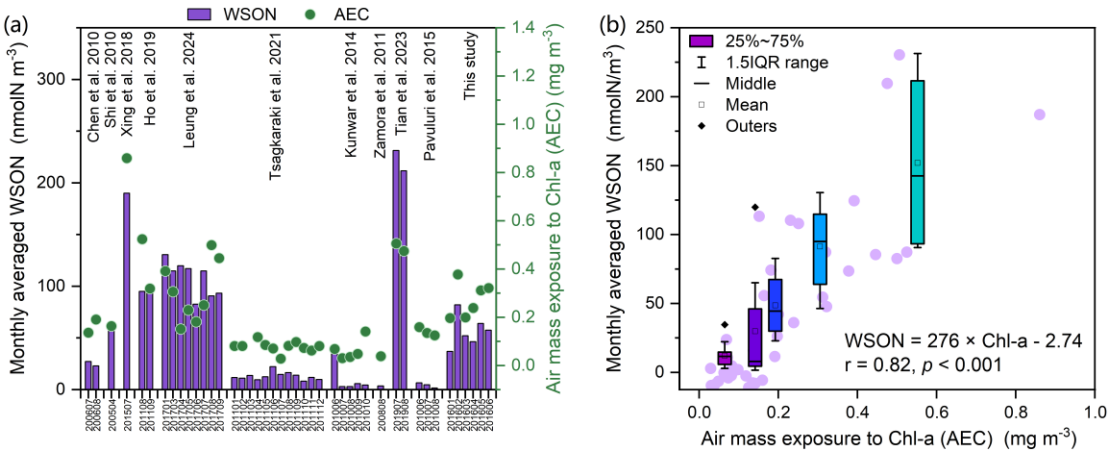

Figure 4. (a) Geographic distributions and (b) correlation between AEC values and monthly mean WSON concentration in coastal regions predominantly influenced by marine air masses. Values are provided in Table S3. Air mass trajectories for these coastal and island sampling sites were recalculated using the HYSPLIT model, and AEC values were derived from MODIS monthly Chl-a concentrations.

4. Conclusions

The equation derived in this study (WSON [nmol m^{-3}] = 276 × AEC [mg m^{-3}] – 2.74) provides an empirical basis for examining the linkage between coastal aerosol water-soluble organic nitrogen (WSON) and oceanic biological conditions along air-mass transport pathways. Our results indicate that sea spray aerosol (SSA)-associated WSON is an important contributor to coastal aerosol WSON under marine-influenced conditions, and its covariation with trajectory-based air-mass exposure to chlorophyll-a (Chl-a) (AEC) is consistent with marine-biogenic enhancement. However, these implications should be interpreted with caution because the present dataset was obtained with seasonally uneven sampling coverage, 24 h integrated filter sampling, and without isotopic constraints that could more directly distinguish marine-biogenic, shipping-related, and continental anthropogenic sources. Future work combining more temporally uniform observations with isotopic and molecular-level characterization is needed to further strengthen source attribution. We therefore suggest that integrating satellite-derived Chl-a data into air mass trajectory analyses may help improve future assessments of marine-related WSON variability.

Code and data availability.

Data are available from the link (https://doi.org/10.17605/OSF.IO/YMJ3F).

Supplement

The supplement related to this article is available online.

Author contributions

Conceptualization: JT. Funding acquisition: JT, SH, SZ, and GZ. Investigation: JT, XW, JW, SL, XG, GuZ, and SB. Methodology: JT, XW, and JW. Project administration: GZ and SZ. Resources: YM, SZ, JL, and GZ. Software: XW, and SL. Supervision: JL, SZ, and GZ. Validation: JT and SZ. Writing (original draft): JT. Writing (review and editing): XW, SH, SZ, and GZ.

Competing interests

The authors declare no competing financial interest.

Acknowledgments

This research has been supported by the National Natural Science Foundation of China (42030715, 42192511, and 42207308), the Alliance of International Science Organizations (ANSO-CR-KP-2021-05), the Guangdong Basic and Applied Basic Research Foundation (2021A0505020017 and 2023B1515020067), the National Science Foundation of Chongqing (CSTB2024NSCQ-MSX0897), and the Postdoctoral Fellowship Program of CPSF (GZC20232684).

References

Altieri, K. E., S. E. Fawcett, A. J. Peters, D. M. Sigman, and M. G. Hastings (2016), Marine biogenic source of atmospheric organic nitrogen in the subtropical North Atlantic, *Proc. Natl. Acad. Sci. U. S. A.*, *113*(4), 925-930. https://doi.org/10.1073/pnas.1516847113.

Altieri, K. E., M. G. Hastings, A. J. Peters, and D. M. Sigman (2012), Molecular characterization of water soluble organic nitrogen in marine rainwater by ultra-high resolution electrospray ionization mass spectrometry, *Atmos. Chem. Phys.*, *12*(7), 3557-3571. https://doi.org/10.5194/acp-12-3557-2012.

Buchanan, P. J., O. Aumont, L. Bopp, C. Mahaffey, and A. Tagliabue (2021), Impact of intensifying nitrogen limitation on ocean net primary production is fingerprinted by nitrogen isotopes, *Nat. Commun.*, *12*(1), 6214. https://doi.org/10.1038/s41467-021-26552-w.

Cape, J. N., S. E. Cornell, T. D. Jickells, and E. Nemitz (2011), Organic nitrogen in the atmosphere — Where does it come from? A review of sources and methods, *Atmos. Res.*, *102*(1), 30-48. https://doi.org/10.1016/j.atmosres.2011.07.009.

Chen, H.-Y., and L.-D. Chen (2010), Occurrence of water soluble organic nitrogen in aerosols at a coastal area, *J. Atmos. Chem.*, *65*(1), 49-71. https://doi.org/10.1007/s10874-010-9181-y.

Cornell, S., K. Mace, S. Coeppicus, R. Duce, B. Huebert, T. Jickells, and L. Z. Zhuang (2001), Organic nitrogen in Hawaiian rain and aerosol, *J. Geophys. Res.-Atmos.*, *106*(D8), 7973-7983. https://doi.org/10.1029/2000jd900655.

Facchini, M. C., et al. (2008), Important Source of Marine Secondary Organic Aerosol from Biogenic Amines, *Environ. Sci. Technol.*, *42*(24), 9116-9121. https://doi.org/10.1021/es8018385.

Gantt, B., N. Meskhidze, M. C. Facchini, M. Rinaldi, D. Ceburnis, and C. D. O'Dowd (2011), Wind speed dependent size-resolved parameterization for the organic mass fraction of sea spray aerosol, *Atmos. Chem. Phys.*, *11*(16), 8777-8790. https://doi.org/10.5194/acp-11-8777-2011.

Geng, X., Y. Mo, J. Li, G. Zhong, J. Tang, H. Jiang, X. Ding, R. N. Malik, and G. Zhang (2020), Source apportionment of water-soluble brown carbon in aerosols over the northern South China Sea: Influence from land outflow, SOA formation and marine emission, *Atmos. Environ.*, *229*, 117484. https://doi.org/10.1016/j.atmosenv.2020.117484.

He, Q., C. Li, K. Siemens, A. C. Morales, A. P. S. Hettiyadura, A. Laskin, and Y. Rudich (2022), Optical Properties of Secondary Organic Aerosol Produced by Photooxidation of Naphthalene under NOx Condition, *Environ. Sci. Technol.*, *56*(8), 4816-4827. https://doi.org/10.1021/acs.est.1c07328.

Ho, K. F., S. S. H. Ho, R.-J. Huang, S. X. Liu, J.-J. Cao, T. Zhang, H.-C. Chuang, C. S. Chan, D. Hu, and L. Tian (2015), Characteristics of water-soluble organic nitrogen in fine particulate matter in the continental area of China, *Atmos. Environ.*, *106*, 252-261. https://doi.org/10.1016/j.atmosenv.2015.02.010.

Ho, S. S. H., L. Li, L. Qu, J. Cao, K. H. Lui, X. Niu, S.-C. Lee, and K. F. Ho (2019), Seasonal behavior of water-soluble organic nitrogen in fine particulate matter (PM2.5) at urban coastal environments in Hong Kong, *Air Qual. Atmos. Health*, *12*(4), 389-399. https://doi.org/10.1007/s11869-018-0654-5.

Ito, A., G. Lin, and J. E. Penner (2014), Reconciling modeled and observed atmospheric deposition of soluble organic nitrogen at coastal locations, *Global Biogeochem. Cycles*, *28*(6), 617-630. https://doi.org/10.1002/2013GB004721.

Jickells, T., A. R. Baker, J. N. Cape, S. E. Cornell, and E. Nemitz (2013), The cycling of organic nitrogen through the atmosphere, *Philosophical Transactions of the Royal Society B: Biological Sciences*, *368*(1621), 20130115. https://doi.org/10.1098/rstb.2013.0115.

Kanakidou, M., et al. (2012), Atmospheric fluxes of organic N and P to the global ocean, *Global Biogeochem. Cycles*, *26*. https://doi.org/10.1029/2011gb004277.

Kunwar, B., and K. Kawamura (2014), One-year observations of carbonaceous and nitrogenous components and major ions in the aerosols from subtropical Okinawa Island, an outflow region of Asian dusts, *Atmos. Chem. Phys.*, *14*(4), 1819-1836. https://doi.org/10.5194/acp-14-1819-2014.

Leung, C. W., X. Wang, and D. Hu (2024), Characteristics and source apportionment of water-soluble organic nitrogen (WSON) in PM2.5 in Hong Kong: With focus on amines,

623 urea, and nitroaromatic compounds, *J. Hazard. Mater.*, *469*, 133899.
624 https://doi.org/10.1016/j.jhazmat.2024.133899.
625 Li, J. J., G. H. Wang, J. J. Cao, X. M. Wang, and R. J. Zhang (2013), Observation of
626 biogenic secondary organic aerosols in the atmosphere of a mountain site in central
627 China: temperature and relative humidity effects, *Atmos. Chem. Phys.*, *13*(22), 11535-
628 11549. https://doi.org/10.5194/acp-13-11535-2013.
629 Li, R., L. Cui, Y. Zhao, H. Fu, Q. Li, L. Zhang, and J. Chen (2019), Size-segregated water-
630 soluble N-bearing species in the land-sea boundary zone of East China, *Atmos. Environ.*,
631 *218*, 116990. https://doi.org/10.1016/j.atmosenv.2019.116990.
632 Li, Y., et al. (2023), Dissecting the contributions of organic nitrogen aerosols to global
633 atmospheric nitrogen deposition and implications for ecosystems, *Natl. Sci. Rev.*, *10*(12).
634 nwad244. https://doi.org/10.1093/nsr/nwad244.
635 Liu, Q., Y. Liu, Q. Zhao, T. Zhang, and J. J. Schauer (2021), Increases in the formation of
636 water soluble organic nitrogen during Asian dust storm episodes, *Atmos. Res.*, *253*.
637 https://doi.org/10.1016/j.atmosres.2021.105486.
638 Liu, X., et al. (2023), Secondary Formation of Atmospheric Brown Carbon in China Haze:
639 Implication for an Enhancing Role of Ammonia, *Environ. Sci. Technol.*, *57*(30), 11163-
640 11172. https://doi.org/10.1021/acs.est.3c03948.
641 Luo, L., S. J. Kao, H. Bao, H. Xiao, H. Xiao, X. Yao, H. Gao, J. Li, and Y. Lu (2018), Sources
642 of reactive nitrogen in marine aerosol over the Northwest Pacific Ocean in spring, *Atmos.*
643 *Chem. Phys.*, *18*(9), 6207-6222. https://doi.org/10.5194/acp-18-6207-2018.
644 Mace, K. A., R. A. Duce, and N. W. Tindale (2003), Organic nitrogen in rain and aerosol at
645 Cape Grim, Tasmania, Australia, *J. Geophys. Res.-Atmos.*, *108*(D11).
646 https://doi.org/10.1029/2002JD003051.
647 Matsumoto, K., H. Kobayashi, K. Hara, S. Ishino, and M. Hayashi (2022), Water-soluble
648 organic nitrogen in fine aerosols over the Southern Ocean, *Atmos. Environ.*, *287*.
649 https://doi.org/10.1016/j.atmosenv.2022.119287.
650 Matsumoto, K., K. Sakata, and Y. Watanabe (2019a), Water-soluble and water-insoluble
651 organic nitrogen in the dry and wet deposition, *Atmos. Environ.*, *218*.
652 https://doi.org/10.1016/j.atmosenv.2019.117022.
653 Matsumoto, K., and K. Yamato (2016), Uncertainties in the measurements of water-soluble
654 organic nitrogen in the aerosol, *Atmos. Environ.*, *144*, 220-225.
655 https://doi.org/10.1016/j.atmosenv.2016.08.061.
656 Matsumoto, K., Y. Watanabe, K. Horiuchi, and T. Nakano (2019b), Simultaneous
657 measurement of the water-soluble organic nitrogen in the gas phase and aerosols at a
658 forested site in Japan, *Atmos. Environ.*, *200*, 312-318.
659 https://doi.org/10.1016/j.atmosenv.2018.12.011.
660 Matsumoto, K., Y. Yamamoto, H. Kobayashi, N. Kaneyasu, and T. Nakano (2014), Water-
661 soluble organic nitrogen in the ambient aerosols and its contribution to the dry deposition
662 of fixed nitrogen species in Japan, *Atmos. Environ.*, *95*, 334-343.
663 https://doi.org/10.1016/j.atmosenv.2014.06.037.
664 Miyazaki, Y., P. Fu, K. Ono, E. Tachibana, and K. Kawamura (2014), Seasonal cycles of

665 water-soluble organic nitrogen aerosols in a deciduous broadleaf forest in northern
666 Japan, *J. Geophys. Res.-Atmos.*, *119*(3), 1440-1454.
667 https://doi.org/10.1002/2013jd020713.
668 Miyazaki, Y., K. Kawamura, J. Jung, H. Furutani, and M. Uematsu (2011), Latitudinal
669 distributions of organic nitrogen and organic carbon in marine aerosols over the western
670 North Pacific, *Atmos. Chem. Phys.*, *11*(7), 3037-3049. https://doi.org/10.5194/acp-11-
671 3037-2011.
672 Nehir, M., and M. Koçak (2018), Atmospheric water-soluble organic nitrogen (WSON) in
673 the eastern Mediterranean: origin and ramifications regarding marine productivity, *Atmos.*
674 *Chem. Phys.*, *18*(5), 3603-3618. https://doi.org/10.5194/acp-18-3603-2018.
675 Norris, G., R. Duvall, S. Brown, and S. Bai (2014), EPA Positive Matrix Factorization (PMF)
676 5.0 fundamentals and User Guide Prepared for the US Environmental Protection Agency
677 Office of Research and Development, *Washington, DC*.
678 O'Dowd, C. D., M. C. Facchini, F. Cavalli, D. Ceburnis, M. Mircea, S. Decesari, S. Fuzzi, Y.
679 J. Yoon, and J.-P. Putaud (2004), Biogenically driven organic contribution to marine
680 aerosol, *Nature*, *431*(7009), 676-680. https://doi.org/10.1038/nature02959.
681 O'Dowd, C., et al. (2015), Connecting marine productivity to sea-spray via nanoscale
682 biological processes: Phytoplankton Dance or Death Disco?, *Sci Rep*, *5*(1), 14883.
683 https://doi.org/10.1038/srep14883.
684 Park, K.-T., K. Lee, T.-W. Kim, Y. J. Yoon, E.-H. Jang, S. Jang, B.-Y. Lee, and O. Hermansen
685 (2018), Atmospheric DMS in the Arctic Ocean and Its Relation to Phytoplankton Biomass,
686 *Global Biogeochem. Cycles*, *32*(3), 351-359. https://doi.org/10.1002/2017GB005805.
687 Pavuluri, C. M., K. Kawamura, and P. Q. Fu (2015), Atmospheric chemistry of nitrogenous
688 aerosols in northeastern Asia: biological sources and secondary formation, *Atmos.*
689 *Chem. Phys.*, *15*(17), 9883-9896. https://doi.org/10.5194/acp-15-9883-2015.
690 Pryor, S. C., and L. L. Sørensen (2000), Nitric Acid–Sea Salt Reactions: Implications for
691 Nitrogen Deposition to Water Surfaces, *J. Appl. Meteorol.*, 39(5), 725-731.
692 https://doi.org/10.1175/1520-0450-39.5.725.
693 Prather, K. A., et al. (2013), Bringing the ocean into the laboratory to probe the chemical
694 complexity of sea spray aerosol, *Proc. Natl. Acad. Sci. U. S. A.*, *110*(19), 7550-7555.
695 https://doi.org/10.1073/pnas.1300262110.
696 Quinn, P. K., T. S. Bates, K. S. Schulz, D. J. Coffman, A. A. Frossard, L. M. Russell, W. C.
697 Keene, and D. J. Kieber (2014), Contribution of sea surface carbon pool to organic
698 matter enrichment in sea spray aerosol, *Nat. Geosci.*, *7*(3), 228-232.
699 https://doi.org/10.1038/ngeo2092.
700 Rinaldi, M., et al. (2013), Is chlorophyll-a the best surrogate for organic matter enrichment
701 in submicron primary marine aerosol?, *J. Geophys. Res.-Atmos.*, *118*(10), 4964-4973.
702 https://doi.org/10.1002/jgrd.50417.
703 Savoie, D. L., R. Arimoto, W. C. Keene, J. M. Prospero, R. A. Duce, and J. N. Galloway
704 (2002), Marine biogenic and anthropogenic contributions to non-sea-salt sulfate in the
705 marine boundary layer over the North Atlantic Ocean, *J. Geophys. Res.-Atmos.*,
706 *107*(D18), AAC 3-1-AAC 3-21. https://doi.org/10.1029/2001JD000970.

Schiffer, J. M., L. E. Mael, K. A. Prather, R. E. Amaro, and V. H. Grassian (2018), Sea Spray Aerosol: Where Marine Biology Meets Atmospheric Chemistry, *ACS Central Sci.*, *4*(12), 1617-1623. https://doi.org/10.1021/acscentsci.8b00674.

Sciare, J., O. Favez, R. Sarda-Estève, K. Oikonomou, H. Cachier, and V. Kazan (2009), Long-term observations of carbonaceous aerosols in the Austral Ocean atmosphere: Evidence of a biogenic marine organic source, *J. Geophys. Res.-Atmos.*, *114*(D15). https://doi.org/10.1029/2009JD011998.

Shi, J., H. Gao, J. Qi, J. Zhang, and X. Yao (2010), Sources, compositions, and distributions of water-soluble organic nitrogen in aerosols over the China Sea, *J. Geophys. Res.-Atmos.*, *115*(D17). https://doi.org/10.1029/2009JD013238.

Sun, Y. L., Q. Zhang, J. J. Schwab, W. N. Chen, M. S. Bae, Y. C. Lin, H. M. Hung, and K. L. Demerjian (2011), A case study of aerosol processing and evolution in summer in New York City, *Atmos. Chem. Phys.*, *11*(24), 12737-12750. https://doi.org/10.5194/acp-11-12737-2011.

Tang, J., et al. (2021), Measurement report: Long-emission-wavelength chromophores dominate the light absorption of brown carbon in aerosols over Bangkok: impact from biomass burning, *Atmos. Chem. Phys.*, *21*(14), 11337-11352. https://doi.org/10.5194/acp-21-11337-2021.

Tang, J., et al. (2024), Long-Emission-Wavelength Humic-Like Component (L-HULIS) as a Secondary Source Tracer of Brown Carbon in the Atmosphere, *J. Geophys. Res.-Atmos.*, *129*(5), e2023JD040144. https://doi.org/10.1029/2023JD040144.

Tian, M., et al. (2023), Seasonal source identification and formation processes of marine particulate water soluble organic nitrogen over an offshore island in the East China Sea, *Sci. Total Environ.*, *863*, 160895. https://doi.org/10.1016/j.scitotenv.2022.160895.

Tripathee, L., S. Kang, P. Chen, H. Bhattarai, J. Guo, K. L. Shrestha, C. M. Sharma, P. Sharma Ghimire, and J. Huang (2021), Water-soluble organic and inorganic nitrogen in ambient aerosols over the Himalayan middle hills: Seasonality, sources, and transport pathways, *Atmos. Res.*, *250*. https://doi.org/10.1016/j.atmosres.2020.105376.

Tsagkaraki, M., C. Theodosi, G. Grivas, E. Vargiakaki, J. Sciare, C. Savvides, and N. Mihalopoulos (2021), Spatiotemporal variability and sources of aerosol water-soluble organic nitrogen (WSON), in the Eastern Mediterranean, *Atmos. Environ.*, *246*, 118144. https://doi.org/10.1016/j.atmosenv.2020.118144.

Violaki, K., J. Sciare, J. Williams, A. R. Baker, M. Martino, and N. Mihalopoulos (2015), Atmospheric water-soluble organic nitrogen (WSON) over marine environments: a global perspective, *Biogeosciences*, *12*(10), 3131-3140. https://doi.org/10.5194/bg-12-3131-2015.

Wang, G. H., et al. (2014), Evolution of aerosol chemistry in Xi'an, inland China, during the dust storm period of 2013; Part 1: Sources, chemical forms and formation mechanisms of nitrate and sulfate, *Atmos. Chem. Phys.*, *14*(21), 11571-11585. https://doi.org/10.5194/acp-14-11571-2014.

Wang, J., et al. (2020), Source apportionment of water-soluble oxidative potential in ambient total suspended particulate from Bangkok: Biomass burning versus fossil fuel

combustion, *Atmos. Environ.*, *235*, 117624. https://doi.org/10.1016/j.atmosenv.2020.117624.

Xie, M., X. Chen, M. D. Hays, M. Lewandowski, J. Offenberg, T. E. Kleindienst, and A. L. Holder (2017), Light Absorption of Secondary Organic Aerosol: Composition and Contribution of Nitroaromatic Compounds, *Environ. Sci. Technol.*, *51*(20), 11607-11616. https://doi.org/10.1021/acs.est.7b03263.

Xing, J., J. Song, H. Yuan, Q. Wang, X. Li, N. Li, L. Duan, and B. Qu (2018), Water-soluble nitrogen and phosphorus in aerosols and dry deposition in Jiaozhou Bay, North China: Deposition velocities, origins and biogeochemical implications, *Atmos. Res.*, *207*, 90-99. https://doi.org/10.1016/j.atmosres.2018.03.001.

Xu, Y., et al. (2020), Aerosol Liquid Water Promotes the Formation of Water-Soluble Organic Nitrogen in Submicrometer Aerosols in a Suburban Forest, *Environ. Sci. Technol.*, *54*(3), 1406-1414. https://doi.org/10.1021/acs.est.9b05849.

Yu, X., et al. (2020), Wet and Dry Nitrogen Depositions in the Pearl River Delta, South China: Observations at Three Typical Sites With an Emphasis on Water-Soluble Organic Nitrogen, *J. Geophys. Res.-Atmos.*, *125*(3). https://doi.org/10.1029/2019jd030983.

Yu, X., et al. (2017), Water Soluble Organic Nitrogen (WSON) in Ambient Fine Particles Over a Megacity in South China: Spatiotemporal Variations and Source Apportionment, *J. Geophys. Res.-Atmos.*, *122*(23), 13,045-013,060. https://doi.org/10.1002/2017JD027327.

Zamora, L. M., J. M. Prospero, and D. A. Hansell (2011), Organic nitrogen in aerosols and precipitation at Barbados and Miami: Implications regarding sources, transport and deposition to the western subtropical North Atlantic, *J. Geophys. Res.-Atmos.*, *116*(D20). https://doi.org/10.1029/2011JD015660.

Zhao, Y., et al. (2026), Evolution of secondary organic aerosol under extremely high humidity conditions in urban areas of southwestern China: Formation and scavenging, *Atmos. Res.*, *327*, 108318. https://doi.org/10.1016/j.atmosres.2025.108318.

Zhou, S., Y. Chen, A. Paytan, H. Li, F. Wang, Y. Zhu, T. Yang, Y. Zhang, and R. Zhang (2021), Non-Marine Sources Contribute to Aerosol Methanesulfonate Over Coastal Seas, *J. Geophys. Res.-Atmos.*, *126*(21), e2021JD034960. https://doi.org/10.1029/2021JD034960.

Zhou, S., Y. Chen, F. Wang, Y. Bao, X. Ding, and Z. Xu (2023), Assessing the Intensity of Marine Biogenic Influence on the Lower Atmosphere: An Insight into the Distribution of Marine Biogenic Aerosols over the Eastern China Seas, *Environ. Sci. Technol.*, *57*(34), 12741-12751. https://doi.org/10.1021/acs.est.3c04382.